

## Accelerated bacterial inactivation obtained by HIPIMS sputtering on low cost surfaces with concomitant reduction in the metal/semiconductor content†

Sami Rtimi,<sup>a</sup> Cesar Pulgarin,<sup>a\*</sup> Oualid Baghriché<sup>a</sup> and John Kiwi<sup>\*b</sup>

Cite this: *RSC Advances*, 2013, 3, 13127

Received 28th March 2013,

Accepted 10th June 2013

DOI: 10.1039/c3ra41528g

[www.rsc.org/advances](http://www.rsc.org/advances)

**Novel ultrathin TiO<sub>2</sub>-Cu nanoparticulate films sputtered by highly ionized pulsed plasma magnetron sputtering (HIPIMS) lead to faster bacterial inactivation compared to more traditional sputtering approaches with an appreciable metal saving. HIPIMS sputtering induces a strong interaction of the TiO<sub>2</sub>-Cu-ions (M<sup>+</sup>) with the polyester surface due to the high fraction and density of M<sup>+</sup>-ions interacting with the biased substrate.**

Antimicrobial surfaces can reduce/eliminate hospital-acquired infections (HAI) acquired on contact with bacteria surviving for long times in hospital facilities.<sup>1,2</sup> To preclude/decrease viral, nosocomial infections and antibiotic resistant bacteria Borkow and Gabbay<sup>3</sup> introduced Cu into textile fabrics. Recently Sunada *et al.*,<sup>4,5</sup> and Irie *et al.*<sup>6</sup> have reported the preparation of the Cu and TiO<sub>2</sub>-Cu films by sol-gel methods and with absorption in the visible range. The sol-gel deposited films are not mechanically stable, in many cases their preparation is not reproducible and do not present uniformity but only low adhesion since they can be wiped off by a cloth or thumb.<sup>7</sup> Films obtained by direct current magnetron sputtering (DC/DCP) as reported avoid the disadvantages of Cu-films prepared by sol-gel methods<sup>4-7</sup> since they deposit uniform and adhesive metal films chemical bonding and mechanical interlocking leading on substrates resisting up to 120–130 °C.

In recent years physical vapour deposition (PVD) has been used to produce antimicrobial films by condensation of a vaporized precursor onto the substrate at relatively high temperatures. Parkin,<sup>8</sup> Foster<sup>9</sup> and Dunlop<sup>10</sup> have reported antibacterial film preparation of Ag and Cu films on glass and thin polymer films by PVD. TiO<sub>2</sub>, Ag, and Cu films 6 to 50 nm thick have been shown to inactivate bacteria under UV and in some cases under visible light irradiation. The disadvantages of the PVD deposition approach are the high investment costs, the high temperatures needed precluding film deposition on textiles besides the large amount

of heat used requiring costly cooling systems. Highly ionized pulsed plasma magnetron sputtering (HIPIMS) has been reported recently able to sputter films applying strong electrical pulses leading to layers presenting superior resistance against corrosion and oxidation.<sup>11</sup> The non-uniform deposition on rugous and complex shape substrates is one of the main problems encountered when depositing uniform Cu-films by direct current pulsed magnetron sputtering (DC/DCP).<sup>12</sup> Cu-polyester has been shown to be effective against Gram-positive *S. Aureus* as reported recently.<sup>13</sup> This study addresses HIPIMS sputtering on polyester leading to ultrathin uniform films showing an accelerated bacterial deactivation due to the induced high energy Cu-ions (M<sup>+</sup>) produced in the magnetron chamber, the HIPIMS plasma density and the increased effect of the applied bias voltage on the Cu-ions (M<sup>+</sup>) compared to DC/DCP sputtering.

HIPIMS deposition of Cu was carried out in a CMS-18 Vacuum system from Kurt Lesker Ltd. using Cu and TiO<sub>2</sub> targets of 50 mm in diameter (K. Lesker Ltd. UK). The TiO<sub>2</sub>-Cu composite target had composition of 60/40 atomic% in TiO<sub>2</sub>-Cu. The HIPIMS was operated at 500 Hz with pulses of 100 ms separated by 1.9 ms, leading to a deposition rate for TiO<sub>2</sub>-Cu of 15.3 nm min<sup>-1</sup>. The average power was 87.5 W (5 A × 350 V) and the power per pulse of 100 ms was 1750 W. In the case of DCP, 622 V and 0.3 A were applied during 3 pulses of 10 ms each, within a 50 ms period. This gives 187 W per period or 62.3 W per pulse and an average power of 312 W per sputtering cycles. The polyester-Dacron terephthalate EMPA test cloth no. 407. 54 spun, 130 microns thick is known for his high mechanical and chemical resistance. Fibers were made of particle sizes <500 nm and present a tensile strength of 75 MPa, refractive index 1.57 an density 1.38 g cm<sup>-3</sup> with a melting point of 250 °C. The 3-D term used to describe the 130 microns thick polyesters fabric addresses the wide misconception that these fabrics are flat and uniform which is not the case, since it is made of fibers 0.3 to 0.5 micron thick. The film thickness was determined with a profilometer (Alphastep500, TENCOR). The X-ray fluorescence (XRF) determination of the Ti-Cu samples was evaluated in a PANalytical PW2400 spectrometer. The *Escherichia coli* (*E. coli*) counting was evaluated according to references<sup>13-15</sup> and the experimental points replicated three times. The statistical

<sup>a</sup>Ecole Polytechnique Fédérale de Lausanne, EPFL-SB-ISIC-GPAO, Station 6, CH-1015, Lausanne, Switzerland

<sup>b</sup>Ecole Polytechnique Fédérale de Lausanne, EPFL-SB-ISIC-LPI, Bat Chimie, Station 6, CH1015, Lausanne, Switzerland

† Electronic supplementary information (ESI) available. See DOI: 10.1039/c3ra41528g

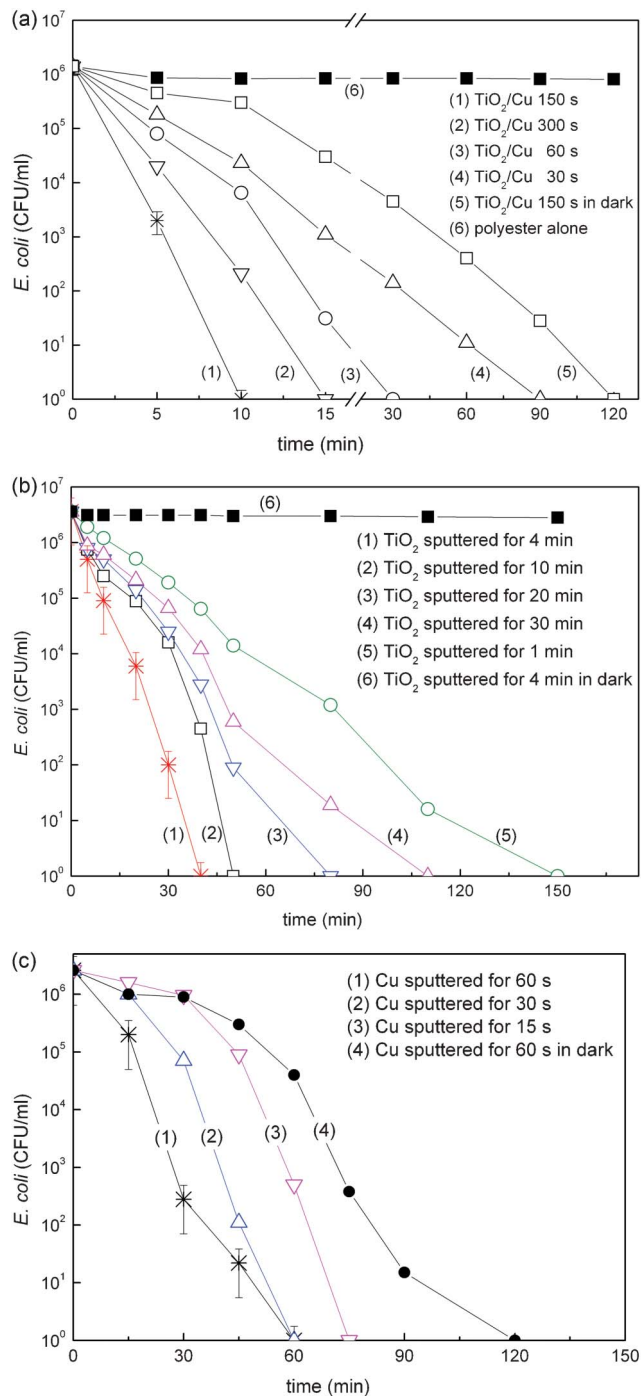
analysis of the results was performed for the decrease of the bacterial CFU values reporting the standard deviation values for the runs showing the fastest bacterial inactivation. Irradiation of the samples was carried out in the cavity of an Osram Lumilux 18 W/827 actinic lamp (400–700 nm, unit emission  $1.3 \text{ mW cm}^{-2}$ ) being 30 cm the distance between the light source and the sample. Transmission electron microscopy (TEM) was carried out in a Philips CM-12 microscope at 120 kV. X-ray Photoelectron Spectroscopy (XPS) used an AXIS NOVA photoelectron spectrometer (Kratos Analytical, Manchester, UK) and the surface atomic concentration of the elements was determined using known sensitivity factors.<sup>16</sup>

Thickness calibrations were carried out for HIPIMS sputtered films on Si-wafers at 5A from a target  $\text{TiO}_2\text{-Cu}$  60%/40% for 150 s leading to the faster bacterial inactivation. The composite film was 38 nm thick for  $\text{TiO}_2\text{-Cu}$  sputtered for 150 s. This is equivalent to  $\sim 190$  layers 0.2 thick nm with  $10^{15}$  atoms  $\text{cm}^{-2}$  per layer deposited at a rate of  $7.6 \times 10^{16}$  atoms/ $\text{cm}^2 \text{ min}^{-1}$ . X-ray fluorescence (XRF) indicated a composition 0.29% wt CuO and a 0.45% wt  $\text{TiO}_2$  per weight polyester.

Under actinic light, Fig. 1a, traces 3, 4 and 5 show the bacterial inactivation as the sputtering time was increased up to 150 s. Sputtering for 300 s induces bacterial inactivation taking longer times than the sample sputtered for 150 s. Therefore, the amount of  $\text{Cu}^0$  is not the main species leading to bacterial inactivation. This sample presents the highest amount of Cu-sites held in exposed positions interacting on the surface or close to the polyester surface with *E. coli* and leading to bacterial inactivation.<sup>12,13</sup> A very high dispersion is attained by sputtering CuO on  $\text{TiO}_2$ . The visible light is absorbed by CuO. We suggest that no  $e^-$  injection is possible from the CuOcb (at  $-0.30 \text{ eV vs. SCE at pH 7}$ ) to the  $\text{TiO}_2\text{cb}$  ( $-0.60 \text{ eV vs. SCE, pH 7}$ ). Also the CuOvb ( $+1.4 \text{ eV}$ ) cannot transfer the CuO holes to the  $\text{TiO}_2\text{vb}$  at 2.5 eV. These energetic considerations lead us to rationalize the fast kinetics reported in Fig. 1a as due to the high CuO dispersion on  $\text{TiO}_2$ .

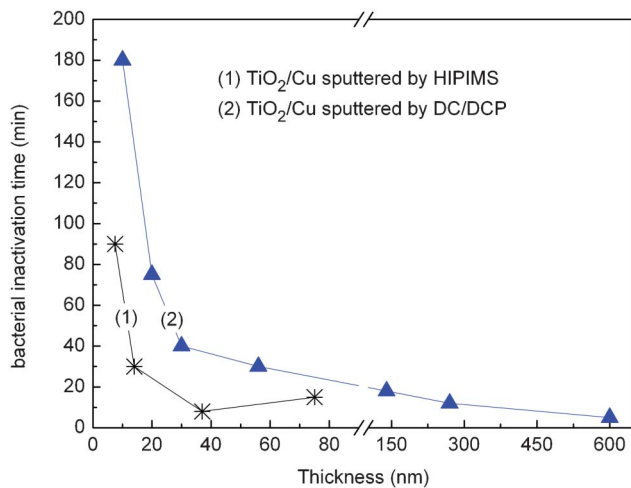
Diffuse reflectance spectroscopy (DRS) show that the absorption in Kubelka–Munk units of the Cu absorption lies between 250 and 650 nm and increases with longer Cu-sputtering times.<sup>14</sup> The DRS intensity was directly related with the bacterial inactivation kinetics times under light irradiation (see Fig. 1a). The Cu-particles present sizes between 8–12 nm. The distribution of  $\text{TiO}_2$  and Cu-nanoparticles was found to be uniform without cracks. The charge transfer between the  $\text{TiO}_2\text{-Cu}$  sample and the *E. coli* depends on the diffusion of the charges on the  $\text{TiO}_2\text{-Cu}$  and this is a function of the particle size.<sup>4,14</sup> Due to its size, the CuO–Cu nanoparticles are not able to penetrate the bacteria cell wall porins with a diameter of 1.1–1.5 nm,<sup>13–15</sup> but Cu-ions are able to diffuse through bacterial porins leading to DNA damage and finally to bacterial inactivation.<sup>2,13</sup> More pathogenic thick walled bacteria like *Staphylococcus aureus* with cell wall  $\sim 40 \text{ nm}$  have been recently reported to be inactivated by Cu-polyester in the dark.<sup>13</sup> Repetitive recycling of the  $\text{TiO}_2\text{-Cu}$  (150 s) samples up to the 8th cycle showed no loss in activity suggesting a stable content of CuO–Cu-ions in the  $\text{TiO}_2$  film.

Fig. 2 presents the inactivation time vs. thickness for DCP and HIPIMS  $\text{TiO}_2\text{-Cu}$  sputtered films. Fig. 2 also shows the significant



**Fig. 1** (a) *E. coli* survival on  $\text{TiO}_2\text{-Cu}$  polyester samples under Osram Lumilux 18 W/827 actinic lamp irradiation ( $4.2 \text{ mW cm}^{-2}$ ). (b) *E. coli* survival on  $\text{TiO}_2$  HIPIMS-sputtered on polyester samples for different times in the dark and under Osram Lumilux 18 W/827 actinic lamp ( $4.2 \text{ mW cm}^{-2}$ ). (c) *E. coli* survival on Cu HIPIMS-sputtered samples for different times in the dark and under Osram Lumilux 18 W/827 light ( $4.2 \text{ mW cm}^{-2}$ ).

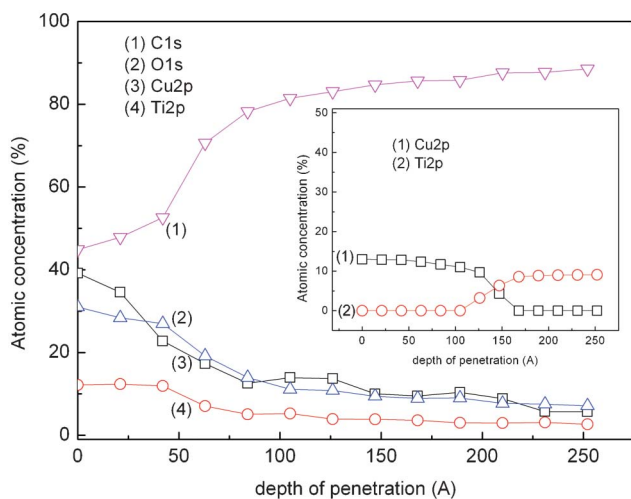
reduction for the HIPIMS  $\text{TiO}_2\text{-Cu}$  layer thickness compared to DC/DCP deposited layer thickness required to inactivate bacteria. The HIPIMS film with a thickness of 38 nm required  $\sim 10$  min to inactivate bacteria compared with a thickness layer of 600 nm



**Fig. 2** Bacterial inactivation time vs. nominal thicknesses for HIPIMS sputtered  $\text{TiO}_2$ -Cu films and DC/DCP sputtered films.

when applying DC/DCP sputtering. To explain the result shown in Fig. 2 the HIPIMS power per pulse was 1750 W/100  $\mu\text{s}$ . This value is significantly higher than the power per pulse applied by DCP of 62.3 W/10  $\mu\text{s}$ . The HIPIMS charge density is two orders of magnitude higher than in DCP and comprising pulses  $\sim 60$  times more energetic than the pulses applied by DCP.

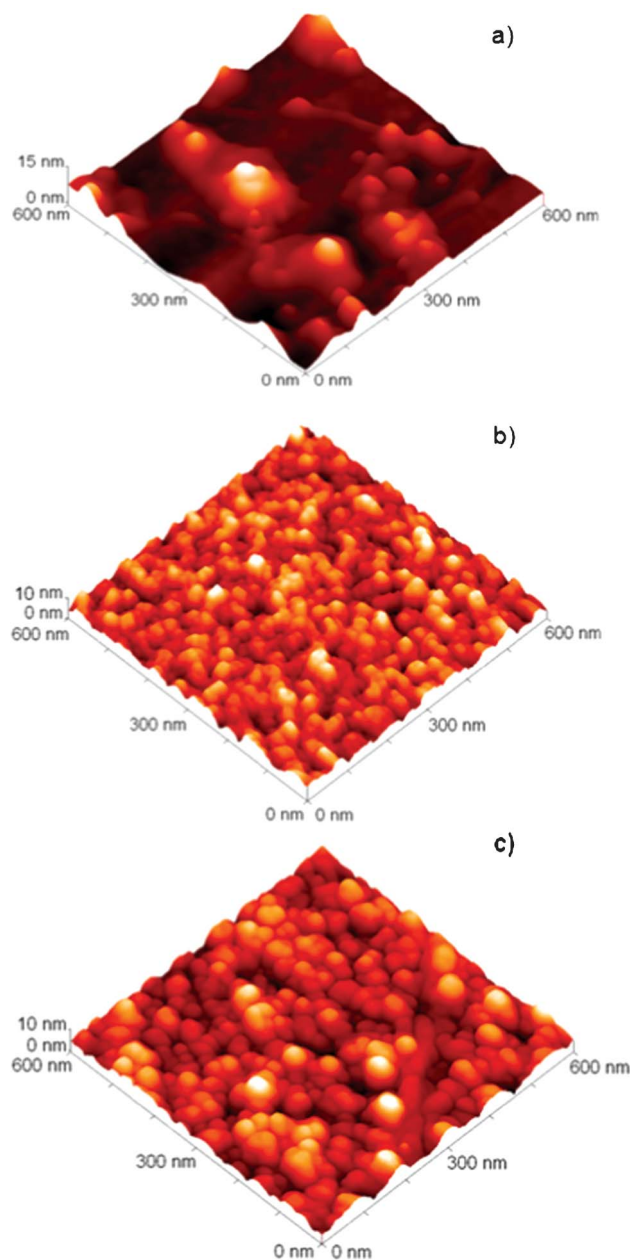
The thinner films deposited by HIPIMS in Fig. 2 show that fast bacterial inactivation kinetics are possible due to the HIPIMS energy increasing the ionization percentage  $\text{M} \rightarrow \text{M}^+$  and leading to the alignment of the  $\text{M}^+$ -ions on the polyester surface.<sup>18,19</sup> The HIPIMS proceeds with a  $\text{M}^+$  ionization level of  $\sim 70\%$  and an electronic density of  $\sim 10^{18-19} \text{e}^- \text{m}^{-3}$  compared to DCP-sputtering with an ionization of  $\text{M}^+ > 5\%$  and an electronic density  $\sim 10^{15-16} \text{e}^- \text{m}^{-3}$ .<sup>11,17</sup> The  $\text{M}^+$ -ions produced in the plasma are attracted to the biased substrate applied on the substrate



**Fig. 3** XPS etching of  $\text{TiO}_2$ -Cu HIPIMS sputtered on polyester showing the penetration of the elements up to 250 Angstroms ( $\sim 120$  atomic layers). Insert: depth profile of  $\text{TiO}_2$ -Cu on polyester sputtered by DCP.

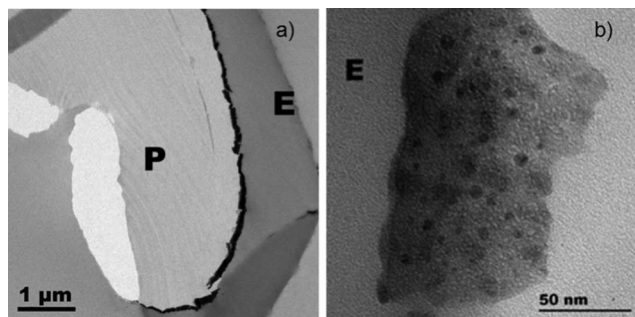
( $-200 \text{ V}$ ). This results in a normal incidence of the  $\text{M}^+$ -ions on the substrate surface re-directing the  $\text{M}^+$ -ion deposition.<sup>19</sup> The applied bias voltage has a more important effect when using HIPIMS sputtering compared to DCP, due to the high charge density generated by HIPIMS in the magnetron chamber.

Fig. 3 presents the atomic percentage concentration of Cu, Ti,  $\text{O}_2$  and C in the sample of  $\text{TiO}_2$ -Cu sputtered for 150 s as a function of  $\text{Ar}^+$  depth penetration. It is readily seen that the concentration of Cu, Ti and O decrease up to 240  $\text{\AA}$ . The penetration of  $\text{Ar}$ -ions was referenced by the standard value of 15 atomic layers of Ta etched per minute ( $\sim 30 \text{\AA} \text{min}^{-1}$ ). The



**Fig. 4** Atomic force microscopy (AFM) of: (a) Cu sputtered with HIPIMS for 150 s ( $\text{rms} = 8.35 \text{ nm}$ ), (b)  $\text{TiO}_2$  sputtered with HIPIMS for 4 min ( $\text{rms} = 3.15 \text{ nm}$ ) and (c)  $\text{TiO}_2$ -Cu sputtered with HIPIMS for 30 s ( $\text{rms} = 5.6 \text{ nm}$ ).





**Fig. 5** Transmission electron microscopy (TEM) of: (a)  $\text{TiO}_2\text{-Cu}$  HIPIMS sputtered for 150 s covers continuously the surface of the polyester fiber and (b)  $\text{TiO}_2\text{-Cu}$  HIPIMS on polyester sputtered for 150 s showing the nanoparticle sizes 8–12 nm.

penetration of the Cu into the polyester protects the Cu-clusters inside the 130  $\mu\text{m}$  thick polyester network during the *E. coli* inactivation process. The increase in the C-content in Fig. 3 was due to the etching removing the  $\text{TiO}_2\text{-Cu}$  layers making available a larger fraction the C-content of the polyester. The insert in Fig. 3 shows the significantly lower atomic concentration percentage of Cu and Ti for  $\text{TiO}_2\text{-Cu}$  sputtered by DC/DCP compared to HIPIMS sputtering. The results in Fig. 3 show the penetration in the polyester of Cu, Ti, C and O on the polyester samples etched by Ar-ions as detected by XPS. The most interesting observation shown in Fig. 3 is the pattern of the Ti, Cu and O profiles when a target with a composition 60/40 atomic%  $\text{TiO}_2\text{-Cu}$  was used for the simultaneous sputtering of Ti and Cu.

Recent studies reported the visible light-sensitive  $\text{TiO}_2\text{-Cu}$  photocatalyst showing interfacial charge transfer (IFCT) leading to the electron transfer from  $\text{TiO}_2\text{vb}$  to  $\text{Cu(II)}$ .<sup>6</sup> In a second more extended study these authors reported the film antibacterial activity was due to  $\text{TiO}_2$  holes in the valence band and  $\text{Cu(I)}$  produced by IFCT in Cu nano-cluster.<sup>20</sup> The interfacial charge transfer would proceed with a considerable driving force induced by the large gap between the  $\text{TiO}_2\text{vb}$  and the  $\text{Cu(II)/CuOvb}$  leading to the fast *E. coli* inactivation times of  $\sim 10$  min shown in Fig. 1a compared to the times noted for the bacterial degradation in Fig. 1b/1c.

Fig. 4 presents the rugosity of the  $\text{TiO}_2\text{-Cu}$ ,  $\text{TiO}_2$  sputtered and Cu sputtered samples inducing the fastest bacterial inactivation. The rugosity of the surfaces are close to each other and are relatively low within the detection limit of the AFM instrument ( $<10$  microns).

The adhesion of the  $\text{TiO}_2\text{-Cu}$  nanoparticles to a polyester fiber is shown in Fig. 5 by Transmission electron microscopy (TEM) for a  $\text{TiO}_2\text{-Cu}$  HIPIMS sputtered sample for 150 s. Continuous coverage of the polyester fiber is seen in Fig. 5a. The  $\text{TiO}_2\text{-Cu}$  nanoparticle sizes 8–12 nm is shown for this sample in Fig. 5b.

## Conclusions

The first evidence is presented for the functionalization of polyester by very thin HIPIMS layers of  $\text{TiO}_2\text{-Cu}$  along the kinetics

and microstructure of these films leading to bacterial inactivation. The bacterial inactivation by the  $\text{TiO}_2\text{-Cu}$  films was faster compared to Cu or  $\text{TiO}_2$  sputtered separately. Savings in metal and deposition time (energy) was attained with HIPIMS compared to conventional DC/DCP-sputtering.

## Acknowledgements

We thank the COST Actions MP0804 and MP1106, the EPFL and LIMPID FEP-7 Collaborative European Project Nanocomposite Materials NMP 2012.2.2.2-6 (N. 310177) for support of this work. We also thank Dr R. Bandorf (Braunschweig, GE) for his help with the HIPIMS work.

## References

- 1 K. Taylor, R. Roberts and J. Roberts, *The challenge of hospital acquired infections (HAI)*, Nat. Audit Office, UK, 2002.
- 2 S. Dancer, *J. Hosp. Infect.*, 2009, **73**, 378–389.
- 3 G. Borkow and J. Gabbay, *J. FASEB*, 2004, **188**, 1728–1730.
- 4 K. Sunada, T. Watanabe and K. Hashimoto, *Environ. Sci. Technol.*, 2003, **37**, 4785–4789.
- 5 H. Irie, S. Miura, K. Kamiya and K. Hashimoto, *Chem. Phys. Lett.*, 2008, **457**, 202–205.
- 6 H. Irie, K. Kamiya, T. Shibanuma, S. Miura, D. Tryk, T. Yokohama and K. Hashimoto, *J. Phys. Chem. C*, 2009, **113**, 10761–10766.
- 7 L. Zhang, R. Dillert and D. Bahnemann, *Energy Environ. Sci.*, 2012, **5**, 7491–7507.
- 8 K. Page, M. Wilson and P. Parkin, *J. Mater. Chem.*, 2009, **19**, 3819–3831 and references therein.
- 9 H. A. Foster, D. W. Sheel, P. Sheel, P. Evans, S. Varghese, N. Rutschke and H. M. Yates, *J. Photochem. Photobiol., A*, 2010, **216**, 283–289.
- 10 P. S. M. Dunlop, P. C. Sheeran, J. A. Byrne, M. A. S. McMahon, M. A. Boyle and K. G. McGuigan, *J. Photochem. Photobiol., A*, 2010, **216**, 303–3010.
- 11 K. Sarakinos, J. Alami and D. Konstantinidis, *Surf. Coat. Technol.*, 2010, **204**, 1661–1684.
- 12 P. Osorio, R. Sanjines, C. Ruales, C. Castro, C. Pulgarin, J.-A. Rengifo, J.-C. Lavanchy and J. Kiwi, *J. Photochem. Photobiol., A*, 2011, **220**, 70–76.
- 13 A. Rio, E. Kusiak, J. Kiwi, C. Pulgarin, A. Trampuz and A. Bizzini, *Appl. Environ. Microbiol.*, 2012, **78**, 8176–8182.
- 14 O. Baghriche, S. Rtimi, C. Pulgarin, R. Sanjines and J. Kiwi, *ACS Appl. Mater. Interfaces*, 2012, **4**, 5234–5240.
- 15 H. Nikaïdo, *J. Biol. Chem.*, 1994, **4**, 3905–3908.
- 16 D. Wagner (Ed), *Handbook of X-ray Photoelectron Spectroscopy*, Perkin-Elmer Corporation Physical Electronics Division, Minnesota, 1979.
- 17 P. Kelly and R. Arnell, *Vacuum*, 2000, **56**, 159–172.
- 18 I. Petrov, L. Hultman, U. Helmersson and J. Sundgren, *Thin Solid Films*, 1989, **169**, 299–314.
- 19 V. Kousznetsov, K. Macak, J. Schneider, U. Helmersson and I. Petrov, *Surf. Coat. Technol.*, 1999, **122**, 290–295.
- 20 X. Qiu, K. Sunada, M. Minoshima, M. Liu, Y. Lu, D. Li, Y. Shimodaira, Y. Hosogi, Y. Kuroda and K. Hashimoto, *ACS Nano*, 2012, **6**, 1609–1618.